FAWSETS: Flow-Driven Arterial Water Stimulation with Elimination of Tissue Signal

KENNETH MARRO

Department of Radiology, University of Washington, Seattle, Washington 98115-7115

Measurements of perfusion with NMR are most commonly achieved through the use of exogenous tracers such as deuterium (*1–5*), fluorine (*1, 4, 6*), or paramagnetic agents (*7–9*). Aside from being invasive, measurements made with these tracers can be difficult to quantify due in part to the problem of relating image contrast to tracer concentration (*8, 10, 11*). Recirculation effects and/or toxicity can preclude the use of exogenous tracers in studies where multiple measurements are to be made on the same subject in a short time period. NMR perfusion measurements can also be made using arterial blood water as an endogenous contrast agent (*12–15*). To make such measurements, a transient magnetic label is applied to the arterial water before it moves into the NMR acquisition volume. Several methods of applying the label to the arterial water have been demonstrated (*12, 14*) but the method which offers the highest signal and the best chance of quantifying perfusion is continuous arterial spin inversion (*16*). This paper describes a novel and improved NMR method of measuring perfusion, which has been given the acronym FAWSETS (*f*low-driven *a*rterial *w*ater *s*timulation *w*ith *e*limination of *t*issue *s*ignal).

With arterial spin inversion, the proper combination of a magnetic field gradient and a B_1 field adiabatically inverts the magnetization of the blood water as it flows through the artery which supplies the tissue of interest. Continuous inversion for approximately five T_1 periods brings the magnetization within the acquisition volume to an attenuated steady state. A measurement of perfusion can be extracted by subtracting the signal acquired after inversion from a control signal, which is acquired with no inversion in the artery (*17–19*).

The concept behind FAWSETS is similar to arterial spin inversion in that the natural flowing motion of the blood is used to generate adiabatic manipulations of the vascular water magnetization. However, with FAWSETS the adiabatic manipulation leaves the blood magnetization in the transverse plane. Instead of becoming inverted in the artery, the blood signal is adiabatically exited as it flows into the sensitive volume of the RF coil used to acquire the signal. The excited spins become spin-locked and, except for $T_{1\rho}$ relax-

ation (*20*), remain transverse as long as they stay within the sensitive volume of the RF coil. Conversely, tissue spins, which are present in the acquisition volume at the beginning of the excitation process, become completely saturated and make no contribution to the acquired signal. The resulting water peak consists exclusively of blood water that has moved into the acquisition volume within a time period on the order of several times $T_{1\rho}$. The acquired signal can be used to measure perfusion *in vivo,* as demonstrated in this paper, and should also be ideal for generating angiographic images.

To understand how FAWSETS works, it is necessary to examine the effective field, B_e, at the entrance to a volume coil during a continuous, low-power RF excitation. There are two components to B_e, a longitudinal component parallel to the z axis and a transverse component perpendicular to the z axis. The longitudinal component, $b_z = B_0 - \omega/\gamma$, is directly proportional to the instantaneous frequency offset, ω, of the spins in the rotating reference frame. The transverse component is defined by B_1, the rotating RF field (*21*).

Figure 1A shows that shimming results in a homogeneous field within the sweet spot of a volume coil but leaves inhomogeneous regions at the edges of the coil. These inhomogeneous regions provide spatial variations in b_z which can serve the same purpose as the applied gradient in an arterial-spin-inversion experiment: modulation of b_z as the blood flows through the vasculature. Figure 1B shows an excitation profile along the z axis of the coil. While this profile does not directly measure the B_1 magnitude, it does demonstrate that B_1 also undergoes transitions at the edges of the coil and remains nearly constant within the sweet spot of the coil.

FAWSETS exploits these spatially varying fields to induce continuous adiabatic excitation of the blood water as it flows into the volume coil. To accomplish this, one need only apply continuous, low-power RF to a well-shimmed volume coil in order to produce a combination of static magnetic fields similar to those of Fig. 1. A few centimeters upstream from the coil, b_z has a magnitude of several hundred hertz while B_1 is essentially zero. The effective field in this region is aligned with the z axis of the magnet and with
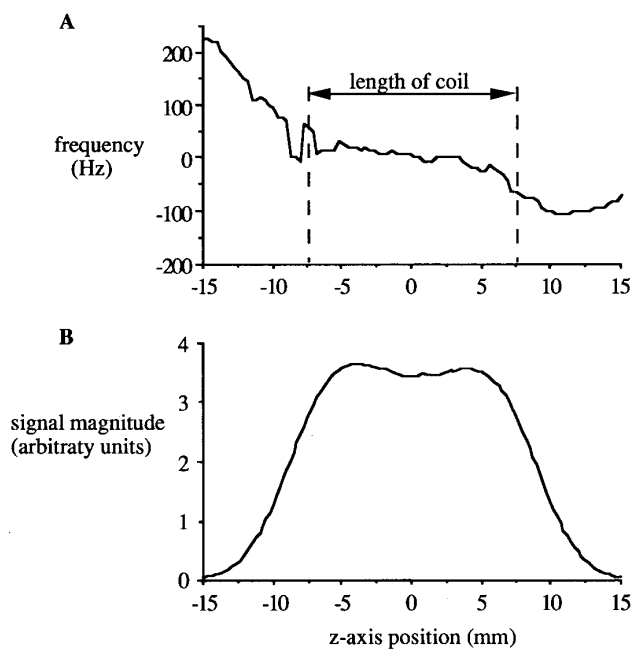
FIG. 1. (A) Spatial variations in the frequency of the water peak. The field inhomogeneity was asymmetric but the adiabatic excitation process was found to work for flow in either direction. The data were acquired with a read gradient along the z axis after a hard pulse followed by a variable delay time. The delay time varied from 0 to 318 ms in increments of 0.25 ms. A 2-D FFT of the resulting data set yielded frequency as a function of position. (B) A z-axis excitation profile acquired after a hard pulse with the delay time set to zero. The profile provides an indication of the spatial distribution of the RF field. The RF power was purposely set high to give a good signal at the edges of the coil; hence, there was a slight dip in the signal at the center of the coil. The data were acquired with a Helmholtz coil with a length of 15 mm and a diameter of 20 mm.

the equilibrium magnetization of the arterial water. As the blood flows toward the coil, b_z decreases and B_1 begins to increase, tipping the effective field away from the z axis. As the blood enters the coil, b_z becomes zero and B_1 reaches a maximum, rotating B_e into the transverse plane. If adiabatic conditions are met during this process, the magnetization of the arterial water will remain aligned with B_e and will also lie in the transverse plane when it enters the coil. Within the sweet spot of the coil, B_e remains constant so the adiabatically excited blood water magnetization will become spin-locked and will remain in the transverse plane until it leaves the coil or until it relaxes according to $T_{1\rho}$.

If the appropriate RF power is applied continuously to the coil for a duration on the order of several times T_1, a steady-state magnetization will develop within the acquisition volume. The water in relatively fast flowing arterial blood will become excited as it moves into the coil volume. It will then either continue through the coil, in which case the magnetization will adiabatically return to a longitudinal orientation and make no contribution to the acquired signal, or it will find its way into capillary beds and diffuse into the tissue,

in which case it will eventually relax according to $T_{1\rho}$. Meanwhile, tissue water which was residing in the homogenous region of the coil at the beginning of the excitation process will be subjected only to a continuous, transverse effective field. It will become completely saturated after about five T_1 periods. A signal acquired with the volume coil can be made to consist exclusively of contributions from freshly perfused arterial water.

Figure 2A provides a graphic demonstration of how effective this adiabatic excitation process is in a simple flow phantom. For this experiment, the flow phantom consisted of a 3 mm inside-diameter tube through which water was pumped at a constant average velocity of 150 mm/s. The phantom was placed at the center of the bore and shimmed using the ''Compu-Shim'' auto-shim routine provided as standard equipment on the Bruker (GE Omega) 4.7 T magnet, version 6.0.3. During an 8 s excitation period, low-power RF, of approximately 60 mG, was supplied continuously to the coil. No additional RF pulses were applied after the excitation period so the projection along the length of the tube reflects the efficacy of the adiabatic excitation process. With the pump turned on, the water becomes excited as it flows into the coil. The velocity is sufficiently high that only minimal relaxation takes place while the water is spin-locked in the homogenous region of the coil. The water remains excited until it leaves the coil. When the pump is turned off, the signal from the nonflowing water in the center of the coil becomes completely attenuated.
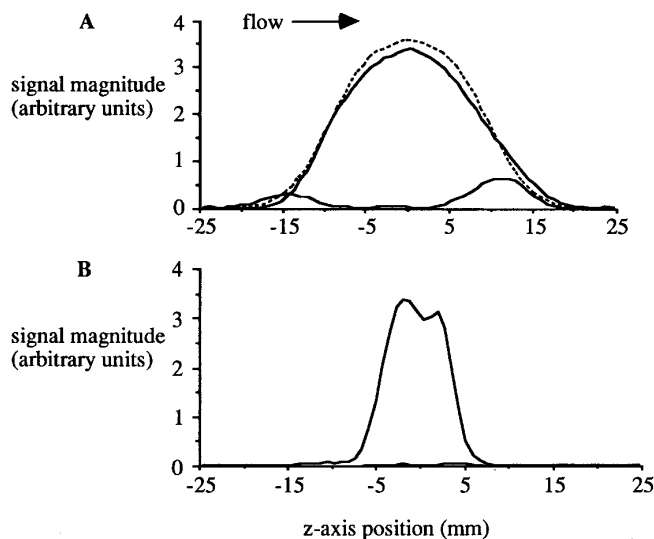

FIG. 2. (A) z-axis profiles acquired from a flow phantom with the flow turned on (upper solid curve) and with the flow turned off (lower solid curve). The profile generated by a hard 90° pulse (dashed curve) is also shown for reference. (B) z-axis profiles from the flow phantom after a soft 180° pulse to select the desired acquisition volume. The upper curve was acquired with the pump turned on, the lower curve was acquired with the pump turned off. The data were acquired with the same coil described in the legend to Fig. 1.

To test repeatability, this flow-phantom experiment was conducted multiple times. Each time the initial shims were set to different values before running the auto-shim routine. Whether the initial shims were all set to zero, to random values, or to the results from a previous auto-shim, the experimental results were essentially the same as in Fig. 2A. In fact, in all the flow phantom experiments undertaken in this study, there has not been a single instance in which the resulting shims did not yield effective adiabatic excitation.

The flow-phantom experiment was also repeated with a wide range of flow rates through the tube. Even at average velocities as high as 1200 mm/s, adiabatic conditions were met and the projections along the length of the tube revealed nearly complete excitation of the flowing spins. As would be expected, at very slow flow rates it was noted that the process was limited by $T_{1\rho}$ relaxation effects. Despite the asymmetry of the field inhomogeneity seen in Fig. 1A, the excitation process worked for flow in either direction in the phantom.

To verify that the results of Fig. 2A were not dependent on the particular coil used, the experiment was also repeated using a different volume coil, one with substantially different dimensions: a diameter of 4.5 mm and a length of 12 mm. The results (data not shown) were essentially the same as those shown in Fig. 2A.

Figure 2A reveals that at the edges of the coil there is a region where the excitation process yields a partial excitation of both the flowing and nonflowing spins. In these regions, the effective field is neither completely transverse nor completely longitudinal. Flowing spins in this region have undergone only a portion of the adiabatic excitation process and only a fraction of the total magnetization of these spins lies in the transverse plane. Nonflowing spins in this region are not completely saturated but instead are brought to a steady state with a small transverse component. This partially excited state is undesirable because it makes the resulting signal difficult to analyze. Fortunately, it is easy to remove this unwanted signal by applying a slice-selective 180° pulse, sandwiched by symmetric gradient pulses, at the end of the adiabatic excitation period. Figure 2B shows the flow-phantom results after application of a slice-selective 180° hyperbolic secant pulse. The combination of the soft 180° pulse and the symmetric gradients removes the signal from outside the selected slice and leaves only the signal from the flowing spins within the acquisition volume.

For *in vivo* perfusion experiments, the 180° pulse and the paired gradients used to select the desired acquisition volume can also provide attenuation of the signal from faster flowing blood in larger arterial vessels and in the venous vessels. If the gradient parameters are properly selected, this ensures that the signal from larger vessels is attenuated and leaves a signal that reflects only perfusion within the acquisition volume. Relative changes in the perfusion signal are clearly demonstrated by the three spectra shown in Fig. 3. These
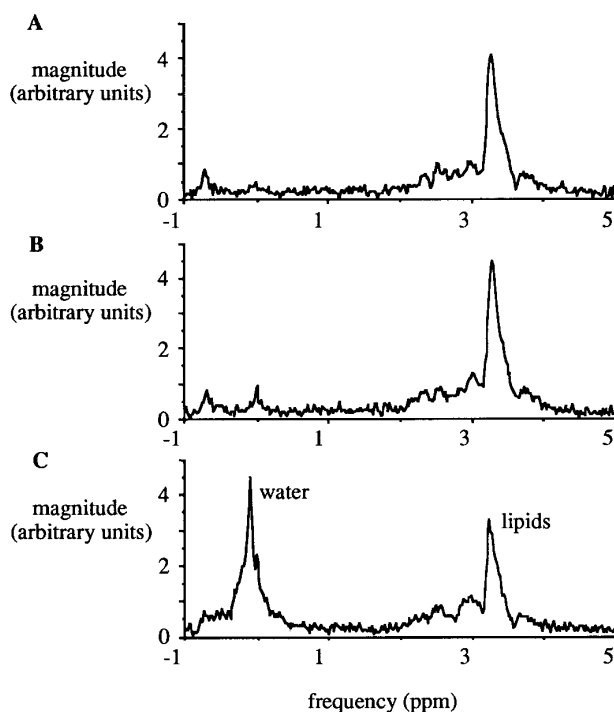

FIG. 3. Examples of magnitude spectra acquired from the muscle tissue in the lower hind limb of a rat under three different conditions: with the femoral artery occluded so that no blood was flowing into the muscle tissue (A); under resting conditions (B); and after three minutes of ischemic exercise (C). The 8 s FAWSETS excitation period was followed by a 180° slice-select pulse (10 mm slice thickness) sandwiched between symmetric gradient pulses. The gradient magnitudes were 0.25 G/mm with durations of 4.0 ms and a separation time of 8 ms.

spectra were acquired from the muscle tissue of the lower hind limb of an anesthetized rat. In spectra such as that in Fig. 3A, which was acquired with the femoral artery occluded and no blood flow to the hind limb, the water signal was almost completely eliminated. In spectra acquired under resting conditions, such as that in Fig. 3B, there was a small, but consistent, water peak reflecting the very low resting perfusion level expected in skeletal muscle. The spectrum in Fig. 3C was preceded by a three-minute ischemic exercise period during which the femoral artery was occluded and the sciatic nerve was stimulated to produce 250 ms tetanic contractions of all the muscles in the lower hind limb every 2 s. The dramatic increase in the area of the water peak in Fig. 3C reflects the large increase in perfusion caused by ischemic exercise.

It is also interesting to note the changes in the lipid signal in the spectra of Fig. 3. The lipid peak was nearly identical under resting and occluded conditions but, after ischemic exercise, the significantly broader peak of Fig. 3C was observed. This effect occurred consistently in the spectra acquired in the early stages of the recovery periods. Numerical integration revealed that the net area of the lipid peak remained essentially constant throughout the experiment (data
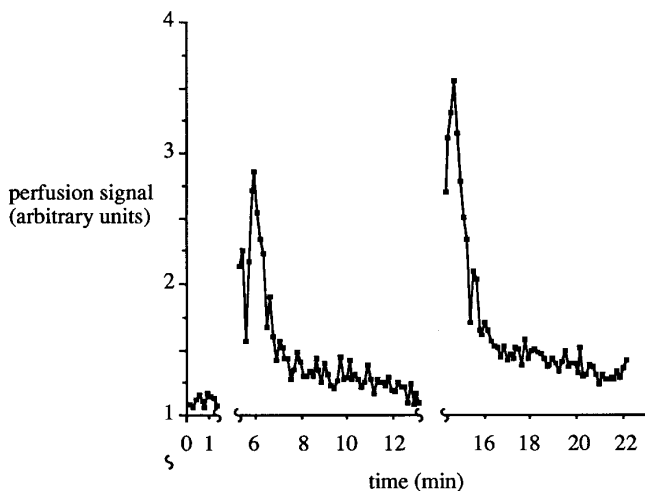
FIG. 4. Two cycles of recovery from ischemic exercise. The first 10 data points were acquired under resting conditions. Each recovery cycle was preceded by a 3 minute ischemic exercise period. The data points represent the area of the water peak as determined by summing points in magnitude spectra.

not shown). Hence, the variations in the lipid signal are limited to a broadening of the peak and most likely reflect changes in susceptibility since large changes in the oxygenation state of the tissue would be expected to occur under this experimental protocol. This observation is important in two respects. First, it indicates that, while susceptibility effects are reflected in the spectra, they do not cause changes in the net areas of the peaks and are unrelated to the large changes in the water peak area. Second, this result suggests that FAWSETS may be used to simultaneously acquire perfusion and susceptibility information, two important and related properties of the tissue.

Figure 4 shows the results from a series of spectra acquired during two periods of recovery from ischemic exercise. Immediately after the exercise period, the perfusion signal increases greatly compared to resting conditions. This large increase is followed by a gradual return to resting levels over a period of about 5 minutes. It should be stressed that no subtraction was necessary to produce the data in this figure. The perfusion signal was extracted by summing the points comprising the water peak in magnitude spectra. In magnitude spectra, the data points are rectified such that none of the data points are less than zero. This can impose a significant bias in the results when points are numerically summed to determine the area of a low amplitude peak. This explains why the perfusion signal in Fig. 4 does not approach zero, even with the femoral artery occluded. Better results would be expected if the data were analyzed using a more robust fitting routine.

The experiment described in Fig. 4 was repeated on three different rats. These experiments showed a consistent perfusion response to ischemic exercise (Fig. 5). The recovery

pattern is the same as that seen in previous experiments in which arterial spin inversion was used to monitor the perfusion response (*22*).

The preliminary results presented in this paper clearly demonstrate the ability of FAWSETS to measure changes in perfusion. FAWSETS requires no exogenous contrast agents or tracers. The procedure is less invasive than deuterium, fluorine, or paramagnetic tracer studies and can be repeated indefinitely without concern for toxicity or recirculation effects. FAWSETS also offers a significant advantage over arterial spin inversion. With FAWSETS no subtraction of signals is required. This eliminates potential errors due to misregistration, reduces the noise introduced by small biological motions, and eliminates artifacts due to susceptibility and blood volume changes which have been observed in arterial spin labeling experiments (*22*). Further, it improves time resolution by a factor of two.

With FAWSETS, the signal from nonflowing tissue water is completely eliminated. The resulting signal exclusively represents water which has moved into the acquisition volume within a time period on the order of several times $T_{1\rho}$. This relatively small water peak can potentially be measured simultaneously with other peaks in the proton spectrum allowing multiple parameters to be measured under identical conditions. For example, in brain tissue, FAWSETS could allow perfusion measurements and spectroscopic imaging to be conducted simultaneously.

It would be premature to rule out the possibility that an unusual feature of the experiments conducted here (e.g., the particular RF coils chosen, the auto-shim routine, or the shape of the B_0 field) is necessary to create the fields required to generate adiabatic excitation of flowing spins. Further research is necessary to fully understand the conditions required for FAWSETS to work consistently and the limitations on its performance. However, the data presented here
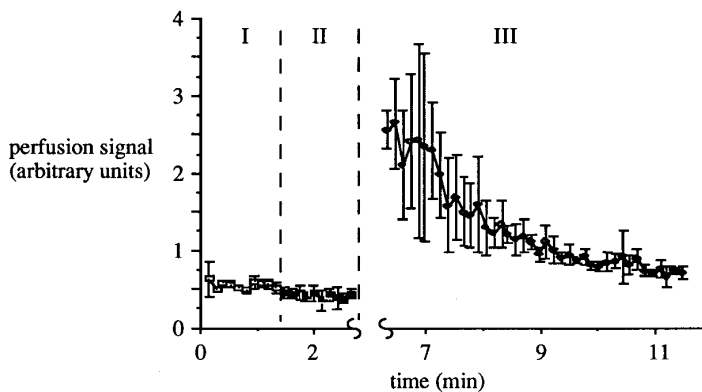

FIG. 5. Combined hind-limb perfusion results from 3 rats. The data are presented as mean ± standard deviation. The first 10 data points were acquired under resting conditions (I). The second 10 data points were acquired with the femoral artery occluded (II). The remaining points were acquired after 3 minutes of ischemic exercise (III).

clearly show that FAWSETS can be made to work. With the aid of a simple model, it should be relatively easy to convert the water peak area in a FAWSETS experiment to a quantitative measure of tissue perfusion. Hence, FAWSETS represents an exciting and significant improvement in the ability to use NMR as a method of imaging large vessel blood flow and for measuring perfusion on a microscopic scale via a macroscopic property.

REFERENCES

1. J. J. Neil, *Magn. Reson. Med.* **19,** 299–304 (1991).

2. J. J. Ackerman, C. S. Ewy, N. N. Becker, and R. A. Shalwitz, *Proc. Natl. Acad. Sci. USA* **84,** 4099–4102 (1987).

3. C. S. Ewy, J. J. Ackerman, and R. S. Balaban, *Magn. Reson. Med.* **8,** 35–44 (1988).

4. S. G. Kim and J. J. Ackerman, *Magn. Reson. Med.* **14,** 266–282 (1990).

5. J. A. Detre, V. H. Subramanian, M. D. Mitchell, D. S. Smith, A. Kobayashi, A. Zaman, and J. S. J. Leigh, *Magn. Reson. Med.* **14,** 389–395 (1990).

6. J. R. Ewing, C. A. Branch, J. A. Helpern, M. B. Smith, S. M. Butt, and K. M. Welch, *Stroke,* **20,** 259–267 (1989).

7. J. W. Belliveau, B. R. Rosen, H. L. Kantor, R. R. Rzedzian, D. N. Kennedy, R. C. McKinstry, J. M. Vevea, M. S. Cohen, I. L. Pykett, and T. J. Brady, *Magn. Reson. Med.* **14,** 538–546 (1990).

8. K. L. Nelson and V. M. Runge, *Top Magn. Reson. Imaging* **7,** 124–136 (1995).

9. V. M. Runge, J. A. Clanton, A. C. Price, C. J. Wehr, W. A. Herzer, C. L. Partain, and A. E. James, *Magn. Reson. Imaging* **3,** 43–55 (1985).

10. R. M. Judd, M. K. Atalay, G. A. Rottman, and E. A. Zerhouni, *Magn. Reson. Med.* **33,** 215–223 (1995).

11. N. Wilke, H. M. Jerosch, A. E. Stillman, K. Kroll, N. Tsekos, H. Merkle, T. Parrish, X. Hu, Y. Wang, and J. Bassingthwaighte, *Magn. Reson. Q.* **10,** 249–286 (1994).

12. K. K. Kwong, D. A. Chesler, R. M. Weisskoff, K. M. Donahue, T. L. Davis, L. Ostergaard, T. A. Campbell, and B. R. Rosen, *Magn. Reson. Med.* **34,** 878–887 (1995).

13. D. A. Roberts, J. A. Detre, L. Bolinger, E. K. Insko, R. E. Lenkinski, M. J. Pentecost, and J. S. Leigh, *Radiology* **196,** 281–286 (1995).

14. D. S. Williams, J. A. Detre, J. S. Leigh, and A. P. Koretsky, *Proc. Natl. Acad. Sci. USA* **89,** 212–216 (1992).

15. W. Zhang, D. S. Williams, J. A. Detre, and A. P. Koretsky, *Magn. Reson. Med.* **25,** 362–371 (1992).

16. E. G. Walsh, K. Minematsu, J. Leppo, and S. C. Moore, *Magn. Reson. Med.* **31,** 147–153 (1994).

17. W. Zhang, D. S. Williams, and A. P. Koretsky, *Magn. Reson. Med.* **29,** 416–21 (1993).

18. W. Zhang, A. C. Silva, D. S. Williams, and A. P. Koretsky, *Magn. Reson. Med.* **33,** 370–376 (1995).

19. D. A. Roberts, J. A. Detre, L. Bolinger, E. K. Insko, and J. S. Leigh, *Proc. Natl. Acad. Sci. USA* **91,** 33–37 (1994).

20. A. Abragam, ''The Principles of Nuclear Magnetism,'' p. 560, Oxford Univ. Press, Oxford, 1961.

21. M. Garwood and K. Ugurbil, *in* ''NMR Basic Principles and Progress'' (P. Diehl, E. Fluck, H. Gunther, R. Kosfeld, J. Seelig, and M. Rudin, Eds.), Vol. 26, pp. 109–147, Springer-Verlag, New York, 1992.

22. K. I. Marro and M. J. Kushmerick, *Magn. Reson. Med.,* in press (1996).